Antineutrino

Related terms:

Electron, Negatron, Proton, Parent, Neutrino, Neutron, Nuclides, Beta Particle, Positron, Gamma Radiation

View all Topics

Tropical Radioecology

Peter Airey, ... John Twining, in Radioactivity in the Environment, 2012

1.2.2.1.1.1 Beta Particle Emission

In general, the emission of a β^-particle (and an electron antineutrino) leads to the conversion of a neutron to a proton within the nucleus. A free neutron can also decay by that process with a half-life of 615 s:

$$n \rightarrow p + \beta^- + \nu_e \text{electronantineutrino} \qquad (1.2)$$

Hence, in the general case, the atomic number (*Z*) is increased and the neutron number (*N*) decreased by one, with no change in the mass number, (*A*= *N*+ *Z*). Beta emission is characteristic of neutron-rich isotopes (i.e., nuclear stability is increased by decreasing the neutron to proton ratio in the nucleus). A well-known example is the beta decay of ^{14}C to ^{14}N (half-life 5730 y):

$$^{14}C \rightarrow {}^{14}N + \beta^- + \nu \quad E_{\beta,max} = 156 keV \qquad (1.3)$$

The rest masses of the ^{14}C and the ^{14}N nuclei are 14.003242 and 14.003074 u, respectively. The decrease in the rest masses is 0.0000168 u (or 156 keV). This is the total energy released during the radioactive decay process, and is known as the $Q_\beta$value. The energy is distributed between the beta particle and the electron antineutrino. The maximum in the β^-energy $E_{\beta,\ max}$corresponds to zero neutrino energy.

This information is encapsulated in radioactive decay schemes. The ^{14}C decay is a particularly simple example as shown in Figure 1.3A. The energy distribution of the emitted beta is depicted in Figure 1.3B.

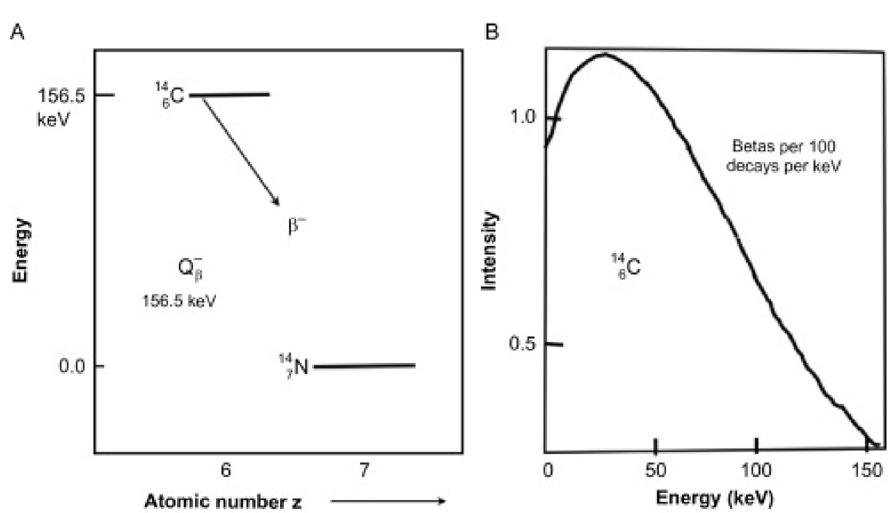

Sign in to download full-size image

Figure 1.3. ^{14}C decay. (A) The ^{14}C decay scheme and energy spectrum. $Q_\beta$is the energy available for decay by the emission of the beta particle (156 keV). (B) The energy spectrum of the emitted beta particles (in units of number of betas per 100 decays per keV.

From http://ie.lbl.gov/decay/betas/BM60014.htm, with permission.

Radiation Physics and Radionuclide Decay

Michael F. L'Annunziata, in Handbook of Radioactivity Analysis (Third Edition), 2012

c Neutrino Mass

Since its inception by Pauli in 1930 up to recent years, the neutrino or antineutrino had been thought to have no rest mass or to possess a near-zero rest mass. It was not until June 5, 1998 that it was announced by the Super-Kamiokande Collaboration, including scientists from 23 institutions in Japan and the United States, at the "Neutrino 98" International Physics Conference in Takayama, Japan, that neutrinos possessed a definite mass (Gibbs, 1998, Kesterbaum, 1998, Kearns et al 1999, and Nakahata, 2000). The mass was not reported, but evidence was provided that the neutrino did possess mass although it was considered to be "very small", at least 0.07 eV, which would be less than a millionth of the electron mass. Evidence for the neutrino mass was provided by demonstrating that neutrinos can "oscillate" from one type into another (*i.e.*, electron-, muon-, and tau-neutrinos) as they travel through space and matter. Oscillation is the changing of neutrino types back and forth from one type to another, and this could occur only if the neutrino possessed mass. Experimental research on neutrino oscillation is reviewed by Messier (2006).

At the "Neutrino 2000" Conference held at Sudbury, Canada June 16–21, 2000, groups from the University of Mainz, Germany (Bonn et al, 2001) and Institute for Nuclear Research, Moscow (Lobashev et al, 2000) reported the mass of the neutrino to be between 2.2 and 2.5 eV/c^2, respectively, at 95% confidence levels. It is common to express subatomic particle mass in units of energy based on equivalence of mass and energy ($E = mc^2$), so that the particle mass m is measured in units of E/c^2 or eV/c^2. Neutrino mass experiments are reviewed by Kraus et al (2005), Otten and Weinheimer (2008), Beck (2010), and Kristiansen (2010). Beck (2010) underscores that results from previous research reported by the Triosk (Russia) and Mainz (Germany) neutrino mass experiments (See Lobashev et al, 1999a,b,c, and 2000, and Kraus et al, 2005) have set the best upper limits of 2.3 eV/c^2 with a 95% confidence limit on the neutrino mass. Beck (1010) also reports that the KATRIN experiment (KArlsruhe TRItium Neutrino experiment) is under preparation to search for the mass of the electron neutrino with a sensitivity of 0.2 eV/c^2. With this objective, the KATRIN experiment will perform a precision measurement of the endpoint region of the β-decay spectrum of tritium, the shape of which depends highly on the neutrino mass. A windowless gaseous tritium source is used in a transport system that guides the beta particles of tritium without energy loss to PIN diode detectors described by Wüstling et al (2006). A pre-spectrometer rejects all beta particles with energy <200 eV below the β-spectrum endpoint, and the beta-particle energies can be measured with a resolution of 0.93 eV. The collection of data to obtain the neutrino mass will start in 2012 and will proceed for five years.

To put the mass of the neutrino in perspective, we can take the current experimental value of the upper limit to the neutrino rest mass, $m_\nu = 2.3$ eV/c^2, and convert this to kilograms as follows:

By definition 1 eV = 1.60×10^{-19} J and, from the equation $E = mc^2$, we can calculate the neutrino rest mass in kilograms as

$$m_\nu=E/c^2=(2.3\,\text{eV})(1.6\times10^{-19}\,\text{J/eV})/(3.0\times10^8\,\text{m/s})^2=4.1\times10^{-36}\,\text{kg} \tag{1.120}$$

If we compare the rest mass of the neutrino, m_ν, to that of the miniscule electron, m_e, we see that the neutrino rest mass is approximately 4 millionths that of the electron or

$$m_\nu/m_e=4.1\times10^{-36}\,\text{kg}/9.1\times10^{-31}=4.5\times10^{-6}$$

Beta Radiation and Beta Decay

Michael F. L'Annunziata, in Radioactivity (Second Edition), 2016

6.2.3 Neutrino Mass

From its inception by Pauli in 1930 up to recent years, the neutrino or antineutrino had been thought to have no rest mass or a near-zero rest mass. But on June 5, 1998 the Super-Kamiokande Collaboration, including scientists from 23 institutions in Japan and the United States, announced at the Neutrino 98 International Physics Conference in Takayama, Japan, that neutrinos possessed a definite mass (Gibbs, 1998; Kesterbaum, 1998; Kearns et al., 1999; Nakahata, 2000). The mass was not reported, but evidence was provided that the neutrino did possess mass although it was considered to be "very small," at least 0.07 eV, which would be less than a millionth of the electron mass.

Evidence for the neutrino mass was provided by demonstrating that neutrinos can "oscillate" from one type or flavor into another (ie, electron-, muon-, and tau-neutrinos) as they travel through space and matter. Oscillation is the changing of neutrino types back and forth from one type or flavor to another; and this could occur only if the neutrino possessed mass. The Nobel Prize in Physics in 2015 was awarded to two key scientists of two large research groups, namely Takaaki Kajita, affiliated with the Super-Kamiokande detector in Japan, and Arthur B. McDonald, affiliated with the Sudbury Neutrino Observatory in Canada, for the discovery of neutrino oscillations as evidence that neutrinos have mass. At the time of the Nobel award, Kajita was director of the Institute for Cosmic Ray Research and professor at the University of Tokyo, Kashiwa, Japan; and McDonald was professor emeritus at Queen's University, Kingston, Canada.

At the Neutrino 2000 Conference held in Sudbury, Canada on 16–21 June 2000, groups from the University of Mainz, Germany (Bonn et al., 2001) and the Institute for Nuclear Research, Moscow (Lobashev et al., 2000) reported the mass of the neutrino to be between 2.2 and 2.5 eV/c^2, respectively, at 95% confidence levels. It is common to express subatomic particle mass in units of energy based on equivalence of mass and energy ($E = mc^2$), so the particle mass m is measured in units of E/c^2 or eV/c^2. Neutrino mass experiments are reviewed by Kraus et al. (2005), Otten and Weinheimer (2008), Beck (2010), and Kristiansen et al. (2010). Beck (2010) underscores that the results from previous research reported by the Triosk (Russia) and Mainz (Germany) neutrino mass experiments (see Lobashev et al., 1999a,b,c, 2000Lobashev et al., 1999aLobashev et al., 1999bLobashev et al., 1999cLobashev et al., 2000; Kraus et al., 2005) have set the best upper limits of 2.3 eV/c^2 with a 95% confidence limit on the neutrino mass. Beck (2010) also reports that the KATRIN (KArlsruhe TRItiun Neutrino) experiment is under preparation to search for the mass of the electron neutrino with a sensitivity of 0.2 eV/c^2. With this objective, the KATRIN experiment will perform a precision measurement of the endpoint region of the β decay spectrum of tritium, the shape of which depends highly on the neutrino mass. A windowless gaseous tritium source is used in a transport system that guides the beta particles of tritium without energy loss to PIN diode detectors, described by Wüstling et al. (2006). A pre-spectrometer rejects all beta particles with energy <200 eV below the β spectrum endpoint, and the beta particle energies can be measured with a resolution of 0.93 eV. The collection of data to obtain the neutrino mass started in 2012 and will continue for 5 years.

To put the mass of the neutrino in perspective, we can take the current experimental value of the upper limit to the neutrino rest mass, $m_v = 2.3$ eV/c^2, and convert this to kilograms as follows.

By definition 1 eV = 1.60×10^{-19} J and, from the equation $E = mc^2$, we can calculate the neutrino rest mass in kilograms as

mv=E/c2=(2.3eV)(1.6×10−19J/eV)/(3.0×108m/s)2=4.1×10−36kg [6.20]

If we compare the rest mass of the neutrino, m_v, to that of the miniscule electron, m_e, we see that the neutrino rest mass is approximately 4 millionths that of the electron, or

mv/me=4.1×10−36kg/9.1×10−31=4.5×10−6

Fundamentals: Physical Methods, Theoretical Analysis, and Case Studies

G.J. Long, in Comprehensive Coordination Chemistry II, 2003

2.6.1 Introduction

Although the neutron is stable when incorporated into a nuclide, a free neutron is unstable and decays into an electron, a proton, and an antineutrino with a half-life of 13 minutes. As a consequence, neutron diffraction experiments must be carried out with neutrons from either a nuclear reactor or a spallation source. In either case the high kinetic energy of the neutrons that result from the nuclear fission or spallation must be reduced, i.e., the neutrons must be thermalized, through collisions with a moderator such as light or heavy water. The resulting thermal neutrons have an energy of ca. 10^{-1} to 10^{-3} eV or a wavelength, as derived from the de Broglie equivalence, of ca. 1–5 Å. Thus thermal neutrons have wavelengths appropriate for diffraction by an atomic or molecular lattice. As a consequence, neutron diffraction is closely related to X-ray diffraction, and typically neutron diffraction studies are preceded by X-ray diffraction structural studies. Neutron diffraction does, however, have certain advantages over X-ray diffraction, advantages which will be discussed herein.

The neutron is a neutral particle that has a nuclear spin of 1/2 and hence a magnetic moment, μ, of −1.913 μ_N, where $\mu_N = eh/2m_p = 5.051 \times 10^{-27}$ J T^{-1} is the nuclear Bohr magneton. A comparison of the fundamental properties of neutrons and X-rays is given in Table 1.

Entropy Principle in the Universe

Ichiro Aoki, in Entropy Principle for the Development of Complex Biotic Systems, 2012

Assuming the existence of black hole evaporation, the following arguements are developed. Then, the universe becomes to consist of only five elementary particles (photon, electron, positron, neutrino, and antineutrino) flying in vacuum (other particles are unstable and decay). Detailed descriptions of these processes are left for various easily accessible books and internet. Reactions of these five elementary particles are reversible, hence no entropy production occurs (Eq. 1.2), i.e., entropy becomes constant. And immediately these elementary particles diffuse to the outside of the universe and the ordered structure in the universe is vanishing, i.e., entropy is growing larger and larger (entropy is a measure of disorder, see Chapter *1.1.1*), i.e., MEP holds in the whole process of the evolution in the universe.

Liquid Scintillation Analysis

Michael F. L'Annunziata, Michael J. Kessler, in Handbook of Radioactivity Analysis (Third Edition), 2012

A Reines and Cowan Reaction

The neutrino remained elusive until 1956, when its existence was demonstrated finally by Nobel Laureate Frederick Reines and Clyde Cowan, Jr. (Reines and Cowan, Jr, 1953, 1956, 1957).

They confirmed the existence of the neutrino using liquid scintillation detectors to demonstrate inverse beta decay where an antineutrino interacts with a proton to yield a neutron and positron, *i.e.*,

$$\bar{\nu}+p^{+}\rightarrow n+e^{+} \qquad (7.131)$$

They constructed a liquid scintillation detector next to a 700-MW nuclear reactor at the Savannah River Plant in Aiken, SC, USA, to detect the abundant antineutrinos emitted by the beta decay of fission products. Their detector was composed of a target chamber consisting of 200 liters of water containing 40 kg of dissolved $CdCl_2$ sandwiched between two tanks of 1400 liters of liquid scintillation solution schematically illustrated in Fig. 7.87. Each end of the scintillator tanks was viewed by 55 photomultiplier tubes (not illustrated). The water provided target protons for the antineutrinos. As illustrated in Fig. 7.87, the interaction of an antineutrino with a water proton would create a neutron (n) and a positron (β^+). The positron would be annihilated when coming to rest and in contact with an electron, and the resulting annihilation radiation (two 0.51-MeV gamma-ray photons emitted in opposite directions) would be detected in coincidence by the two liquid scintillation detectors above and below the water tank (Fig. 7.87). The neutron produced by the antineutrino interaction would slow down quickly (~10 μsec) in the water and be captured by a cadmium nucleus in the water target chamber. The characteristic multiple gamma rays following the neutron capture would be detected in coincidence by the two liquid scintillation detectors. The antineutrino signature therefore consisted of a delayed coincidence between the prompt scintillation pulses produced by the β^+ annihilation and the scintillation pulses produced microseconds later by the neutron capture in cadmium. With the unique signature for the antineutrino provided by the detector design devised by Reines and Cowan, the high neutron flux produced by the Savannah River reactor ($1.2 \times 10^{13}/cm^2$ sec), and reduced cosmic ray backgrounds from massive shielding 11 meters from the reactor and 12 meters underground were essential to the success of their experiment. Nevertheless, a detector running time of 100 days over a period of about one year was required to provide sufficient conclusive signals from the antineutrino signature.

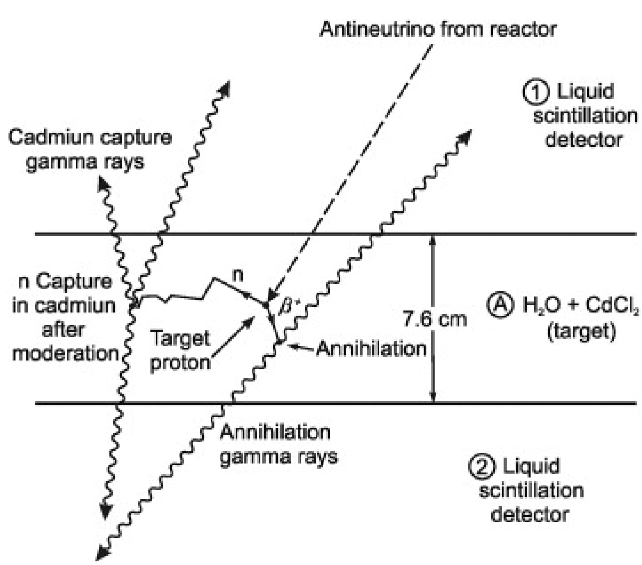

Sign in to download full-size image

FIGURE 7.87. Detection scheme used by Reines and Cowan for the antineutrino signature signal (from Reines, 1995, Nobel Lecture with permission from The Nobel Foundation ©1995). An antineutrino is illustrated entering the tank of aqueous $CdCl_2$ solution and striking a target proton. The proton converts to a neutron and positron. The positron annihilates on an electron with the emission of two 0.511-MeV gamma rays in opposite directions detected by the liquid scintillator in tanks above and below the water target tank. The neutron produced by the antineutrino interaction slows down in the water and is captured by a cadmium nucleus, and the resulting gamma rays are detected by the liquid scintillator in the adjacent tanks approximately 10 microseconds after the positron annihilation.

A more complete account of Pauli's hypothesis of the existence of the neutrino and the work of Reines and Cowan, which culminated in the discovery of the neutrino, is provided in a previous book by the author (L'Annunziata, 2007).

The Atomic Nucleus

Michael F. L'Annunziata, in Radioactivity (Second Edition), 2016

20.11.3.2 Nuclear Recoil from Beta Emissions

Let us calculate the recoil energy imparted to a nucleus by the emission of a beta particle. The following decay of ^{109}Pd by beta particle emission may serve as an example:

$$^{109}_{46}\mathrm{Pd} \rightarrow {}^{109m}_{47}\mathrm{Ag} + \beta^- (E_{max} = 1.03\,\mathrm{MeV}) + \bar{\nu} + \gamma \qquad [20.111]$$

Beta particles are emitted with a broad spectrum of energies, from zero to E_{max}, because the decay energies are shared with a neutrino. We will select the maximum energy (1.03 MeV) that the negative beta particle may possess when the antineutrino energy is at its minimum (near zero) to calculate the maximum recoil energy that the particle may impart to the nucleus. We will not calculate here any nuclear recoil energy that the gamma ray may impart to the nucleus. Again, as in the previous example, the nucleus that undergoes the recoil is that of the daughter nuclide, because it is the daughter that is produced when the beta particle is emitted from the nucleus. Also, we will use the relativistic expression of the recoil energy (Eq. [20.96]) for the calculation. Relevant data from nuclear reference tables for the calculation is the mass of the beta particle (ie, electron mass) and that of ^{109m}Ag, which are 0.000548579 u and 108.904756 u, respectively. The nuclear recoil energy is calculated as

$$K_N = \sqrt{K_p^2 + 2m_pc^2K_p + m_N^2c^4} - m_Nc^2 = \sqrt{\{(1.03\times10^6\,\mathrm{eV})^2 + 2(5.48579\times10^{-4}\,\mathrm{u})(931494013\,\mathrm{eV/u})(1.03\times10^6\,\mathrm{eV}) + [(108.904756\,\mathrm{u})(931494013\,\mathrm{eV/u})]^2\}} - (108.904756\,\mathrm{u})(931494013\,\mathrm{eV/u}) = 10.41\,\mathrm{eV} \qquad [20.112]$$

As we see from this example, the previous example, and Table 20.5, the energies imparted by the massive alpha particles to recoil nuclei are measured in tens of thousands of electron volts, whereas energies imparted by the relatively miniscule beta particle range mostly from a few to several hundred electron volts, and energies imparted to nuclei by gamma-ray and X-ray photons and neutrino emissions are yet smaller.

The Atom as We Know and Use It

Michael F. L'Annunziata, in Radioactivity (Second Edition), 2016

22.3.2 The Weak Force

The weak force, also referred to as the weak nuclear force or weak interaction, is the controlling force involved in charged current and neutral current interactions, including beta decay, as described in detail in Hall of Fame, Part IX of this book. Beta decay involves the conversion of a neutron and proton in the atomic nucleus. Therefore, the distance or range of the weak force is short (10^{-18} m), ie, not exceeding the diameter of a proton or neutron. Because of the very short distance of interaction, it is called the weak force or weak interaction, although it is stronger than gravity (see Table 22.2). With a strength of 10^{-6} relative to the strong nuclear force, the weak force is weaker than the electromagnetic force.

The $W^\pm$ and Z^0 bosons are the mediating particles of the weak force. An example is where the $W^\pm$ boson mediates the weak force in beta decay, which results in either negatron or positron emission. Beta decay with negatron (e^-) emission involves the conversion of a neutron into a proton, as described in the chapter entitled "Beta Radiation and Beta Decay." In this beta decay process, a neutron converts into a proton when a down quark (d) of the neutron transforms into an up quark (u), as illustrated in the Feynman diagram in Fig. 22.6. The conversion of the down quark to an up quark involves the emission of the W^- boson as the exchange particle, which decays into a negative electron (ie, negatron, symbolized as e^- or β^-) and antineutrino (νe^-). The Feynman diagram in Fig. 22.6 illustrates a neutron which contains three quarks, ie, one up quark and two down quarks (udd), transforming into a proton which also contains three quarks, ie, two up quarks and a down quark (uud). In the process, a W^- boson is emitted, which decays into a negative electron (e^-), also known as a negatron or negative beta particle (β^-), and an electron antineutrino (νe^-). A negatively charged boson (W^-) mediates the negatron (β^-) emission, to balance the creation of the positively charged proton from the neutral charge of the original neutron. Thus a negatively charged electron is emitted.

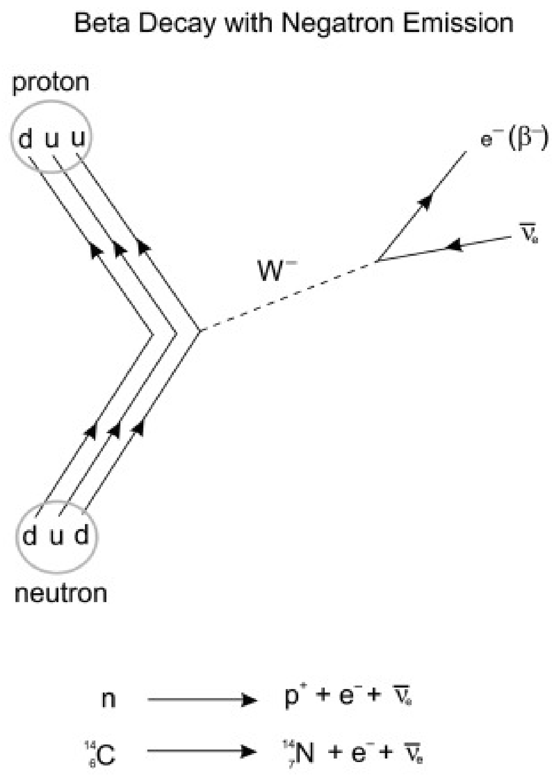

Sign in to download full-size image

Figure 22.6. Feynman diagram illustrating beta decay with negatron emission where a neutron converts to a proton with the emission of a negative electron (beta particle) and an antineutrino. An example is provided by the beta decay of ^{14}C to ^{14}N. The diagram is read from left to right in the direction of the arrows as follows: a d quark of a neutron transforms into a u quark, whereby the neutron then becomes a proton with the emission of a W^- boson which acts as a field exchange particle for the creation and emission of a negative electron, also referred to as a negative β particle or negatron, and the emission of an antineutrino. Antiparticles are illustrated with an *arrow* in the opposite direction.

In the case of beta decay resulting in positron (e^+ or β^+) emission, the antiparticle of the W^-, which is denoted as W^+, is the mediating particle or, in other words, the field particle, ie, the force-carrying particle. This is the particle that carries the energy and momentum from one particle to another, as illustrated in Fig. 22.7. This beta decay process is the opposite of that described in the previous paragraph, and proceeds as follows. A proton, which has a quark composition of one down quark and two up quarks (duu), converts into a neutron, which has a quark composition of two down quarks and one up quark (dud), when an up quark (u) changes into a down quark (d), as illustrated in Fig. 22.7. In the process, a positively charged W^+ boson is emitted as the carrier of this weak force, which balances the positive charge lost in the conversion of the proton to the neutron; and a positive electron (e^+), ie, positron (β^+), is emitted.

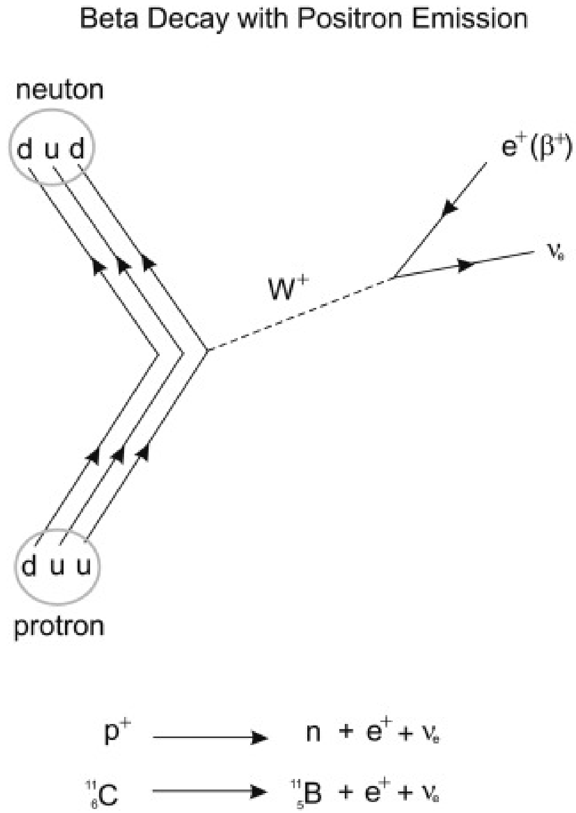

Sign in to download full-size image

Figure 22.7. Feynman diagram illustrating beta decay with positron emission, where a proton converts to a neutron with the emission of a positive electron (ie, positive β particle or positron) and a neutrino. An example is provided by the beta decay of ^{11}C to ^{11}B.

The lifetimes of the $W^{\pm}$ bosons are very short ($\sim 10^{-25}$ s), as they are massive particles (80.3 GeV/c^2) with a mass much greater than that of the proton or neutron. The short lifetime of these particles render them undetectable in beta decay measurements. Taking into account the very large mass of the $W^{\pm}$ bosons, their maximum range can be estimated on the basis of the Heisenberg uncertainty principle to be only 10^{-18} m (according to Eq. [VI.20] of Hall of Fame, Part VI of this book). The equation and calculation of the estimated range are as follows.

For the $W^{\pm}$ bosons with a mass of 80 GeV/c^2, the maximum range of travel would be calculated as

$$d = c\Delta t = c\left(\frac{\hbar}{2m_W c^2}\right) = 2.99\times10^8\,\mathrm{m/s}\left(\frac{6.582\times10^{-22}\,\mathrm{MeV\,s}}{2(80\times10^3\,\mathrm{MeV}/c^2)c^2}\right) = 0.12\times10^{-17}\,\mathrm{m} \approx 1\times10^{-18}\,\mathrm{m}$$

Inverse beta decay, which involves the interaction of a neutrino with a neutron or antineutrino with a proton, is described in the chapter entitled "Beta Radiation and Beta Decay." This phenomenon is commonly used in the detection of neutrinos. The reactions of inverse beta decay (see reactions II.19 and II.20 of Hall of Fame, Part II of this book) involve the conversion of quark flavor with the transformation of a proton to a neutron, or vice versa, a neutron to a proton, and the $W^{\pm}$ bosons as field particles.

All forms of beta decay, including the rare double-beta (ββ) decay, are also mediated by W^- bosons, as illustrated in Fig. 6.13 of Chapter "Beta Radiation and Beta Decay."

The Z^0 boson possesses a neutral charge and a mass of approximately 92 GeV/c^2. Because of its neutral charge, the Z^0 boson is a field particle that mediates or transfers neither charge nor mass in particle interactions. Such interactions are referred to as **neutral current** (NC) weak interactions, such as the neutrino-electron scattering reaction illustrated in Fig. 22.8, which is an interaction used to detect solar neutrinos in liquid scintillation detectors. Another neutral current reaction involving the Z^0 boson, used to detect solar neutrinos, is that which occurs when a neutrino reacts with a deuterium nucleus, whereby neither a proton nor neutron of the deuterium nucleus changes identity. Rather, the combined neutron and proton of the deuterium nucleus separate, as described by the following:

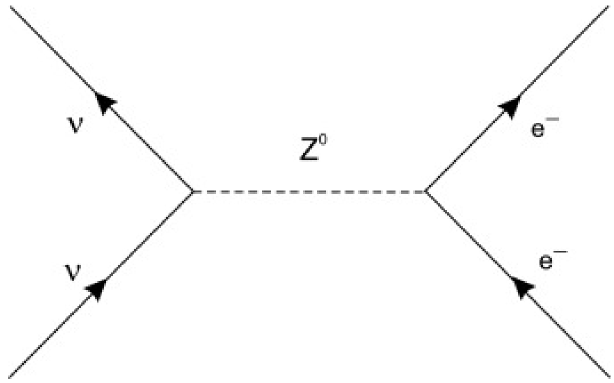

Sign in to download full-size image

Figure 22.8. A Feynman diagram illustrating the mechanism by which a Z^0 boson acts as the field particle or force exchange particle in the interaction of a neutrino with an electron, resulting in an elastic scattering reaction. The interacting neutrino imparts kinetic energy to the electron, resulting in neutrino-electron scattering.

ν+d→Z0p+n+ν

Contrary to neutral current interactions, the $W^{\pm}$ bosons are field particles that mediate **charged current** (CC), where either the W^+ or W^- carries and transfer charge, as illustrated in Figs. 22.6 and 22.7.

$W^{\pm}$ and Z^0 bosons are virtual particles of high mass of approximately 80 and 92 GeV/c^2, respectively. They are very short-lived (approximately 10^{-25} s) and may be considered as photons, which acquire mass as exchange particles via the Higgs mechanism. The same concept holds for the origin of mass of protons and neutrons. The mass of protons (938 MeV/c^2) and neutrons (939 MeV/c^2) represents the principal source of the mass of all matter, as these nucleons constitute the heart of matter. The surrounding electrons of the atom are of relatively very low and almost negligible mass (0.51 MeV/c^2) compared to the mass of the proton and neutron. The protons contain three quarks (duu) with a total mass of only ∼9 MeV/c^2, and neutrons contain three quarks (ddu) with a total mass of ∼10 MeV/c^2. Thus quarks contribute ∼9 MeV/938MeV ≈ 1% of the total mass of protons and ∼10 MeV/939MeV ≈ 1% of the total mass of neutrons. The remaining 99% of the mass of the protons and neutrons is attributed to energy ($E = mc^2$) of the massless gluons, which are emitted and absorbed constantly by the quarks within the protons and neutrons. This binding energy of the massless gluons is the source of ∼99% of the mass of all matter in the universe acquired through the Higgs mechanism.

Solid Scintillation Analysis

Michael F. L'Annunziata, in Handbook of Radioactivity Analysis (Third Edition), 2012

XII Neutrino Interactions

As discussed in Chapter 1, the neutrino is an elusive particle of zero charge and very low mass. The detection and measurement of neutrinos are traditionally carried out with very large masses of liquid scintillators (see Chapter 7), which can provide tons of target material. Examples are the KamLAND detector, which is a 1-kiloton liquid scintillator antineutrino detector, and Borexino, which is a 300-ton liquid scintillator solar neutrino detector, among others discussed in detail in Section XII of Chapter 7.

Solid scintillators including inorganic crystal scintillators have not yet been found to be as useful for the detection and measurement of neutrinos, because of the large mass of target material needed and the difficulty of fabricating inorganic scintillator crystals to very large size and mass. Nevertheless, a large 500-kg CsI(Tl) detector is under development for the detection and measurement of nuclear reactor anti-neutrinos near the core of the Kuo-sheng Nuclear Power Station in Taiwan. Nuclear power reactors are an abundant source of electron anti-neutrinos (ν¯e) in the low-energy (MeV) range. The work is a collaboration mainly between China and the USA, referred to as the TEXONO Collaboration, which is described in detail by Wong and Li (1999), Wong and Li (2000), Li et al. (2001), Lai et al. (2001), Liu et al. (2002), and Zhu et al. (2006). More than one detector may be utilized inside an inner target volume, and one of the detectors is an array of CsI(Tl) crystal scintillators illustrated in Fig. 16.82. The detector, consists of about 510 kg of CsI(Tl) crystals (Unique Crystals, Beijing) arranged in a 17 × 15 matrix with each crystal module weighing ~2 kg. The individual CsI(Tl) crystal modules are hexagonal in shape with a length of 40 cm and the side measuring 2 cm. Photomultiplier tubes (PMTs) are situated at both ends of each module for scintillation light readout, whereby the sum of the two PMT signals ($Q_{tot} = Q_1 + Q_2$) can provide the energy of the event and the difference of the two signals can provide the longitudinal position of the event. The PMT signals are received by amplifiers and shapers, and then digitized by a flash analog digital converter (FADC). Pulse shape analysis is possible to discriminate between pulse events produced by heavy charged particles, such as alpha particles, and those produced by electrons from γ events in the crystal.

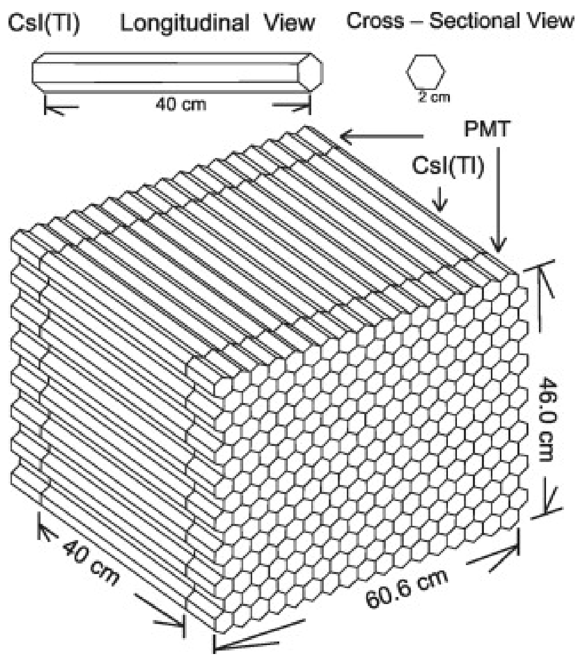

Sign in to download full-size image

FIGURE 16.82. Schematic of the CsI(Tl) target configuration.

(From Zhu et al., 2006; reprinted with permission from Elsevier © 2006)

The compact and massive (~500 kg) CsI(Tl) detector enables sufficient shielding to be built around it including an outer plastic scintillator cosmic-ray veto, 15 cm of lead and 5 cm of steel to shield against ambient background radioactivity, 25 cm of boron-loaded polyethylene to absorb cosmic-ray-induced neutrons, and a dry-nitrogen outer atmosphere sealed in plastic to prevent radon gas from diffusing into the target region. Liu et al. (2002) describes advantages of the CsI(Tl) detector when compared to the conventional liquid scintillation detector, in addition to its compactness described above. These are the following:

1 a large γ-ray photon attenuation of the crystal detector due to its high-*Z* nuclei and density, particularly in the low-energy range below 500 keV. For example, the attenuation length for a 100-keV γ-ray is only 0.12 cm in the CsI(Tl) detector, whereas in a liquid scintillator it would be 6.7 cm. Thus, at this low γ-ray energy, 10 cm of CsI(Tl) detector would have the same attenuation power as 5.6 m of liquid scintillator.

2 a characteristic detector response, that is, the energy resolution of the CsI(Tl) detector is better than a typical liquid or plastic scintillator, and the low-energy γ-ray photons in the crystal scintillator would be fully stopped.

The major event that would be measured in the CsI(Tl) detector are neutrino-electron scattering, which is described in Chapter 7, Section XII.B. The electron antineutrinos originating from the decay of reactor fission products interact with electrons in the CsI(Tl) detector via the elastic scattering reaction

$$\bar{\nu}_e + e^- \rightarrow \bar{\nu}_e + e^- \tag{16.44}$$

due to charged current (CC) and neutral (NC) weak current interactions. The scattered electron can receive any kinetic energy from the neutrino less than or equal to the kinetic energy of the neutrino (Kraus, 2006). Experimentally, the recoil energies of the electrons from the neutrino interactions can be measured in the scintillator, and experimental searches for the neutrino magnetic moment will focus on the reduction in the threshold for the recoil electron energy (Li et al., 2001).

Other electron antineutrino interactions that can be expected with the CsI(Tl) detector are inverse beta decay with ^{133}Cs and ^{127}I. Inverse beta decay is discussed in detail in Section VIII.B of Chapter 1 and Section XII of Chapter 7, which is described by the following:

$$\bar{\nu}_e + p^+ \rightarrow n + \beta^+ \tag{16.45}$$

which is similar to the reaction illustrated in Eq. 1.111 of Chapter 1. Inverse beta decay results in a reduction in atomic number of the isotope be it ^{133}Cs or ^{127}I according to the following:

$$\bar{\nu}_e + (A,Z) \rightarrow (A,Z-1)^* + \beta^+ \quad (16.46)$$

The positron yields a prompt signature with the emission of 511 keV annihilation photons. Characteristic gamma lines from the daughter nuclides are additional signatures. Li et al. (2001) note that with CsI(Tl) as the active target, the gamma lines with M1 transitions would be 81 and 160 keV for ^{133}Cs and 58, 202, and 418 keV for ^{127}I. These would be observed in the pulse height spectra from the CsI(Tl) detector.

Bressi et al. (2001) and Antonini et al. (2001) proposed the use of Yb-doped $Y_3Al_5O_{12}$ (YAG:Yb) scintillator for the detection of low-energy neutrinos, which would react with the ^{176}Yb as follows:

$$\nu_e + {}^{176}Yb \rightarrow {}^{176}Lu^* + e^- \; (Q = 301\,keV) \quad (16.47)$$

$$ {}^{176}Lu^* \rightarrow {}^{176}Lu + \gamma \; (E_\gamma = 72\,keV) \quad (16.48)$$

They note that the signature for this neutrino event is a prompt electron and delayed gamma signal, and to have good discrimination against background noise, a delayed coincidence within 50 ns is required as well as high light yield. The asterisk in Eqns 16.47 and 16.48 denote an excited state of ^{176}Lu. The neutrino reaction with ^{176}Yb differs from that of reactions described by Eqns 16.45 and 16.46, as the neutrino reacts with a neutron resulting in an increase in atomic number, as described in Chapters 1 and 7Chapter 1Chapter 7, according to the following:

$$\nu_e + n \rightarrow p^+ + e^- \quad (16.49)$$

$$\nu_e + (A,Z) \rightarrow (A,Z+1) + e^- \quad (16.50)$$

Tests on YAG:Tb crystals with as much as 15% Yb have been tested by Bressi et al. (2001) and Antonini et al. (2001). They demonstrated a fluorescence time of approximately 10 ns and a light yield of 8000 photons/MeV, which would be suitable for neutrino detection. Several investigations on the scintillation properties of Yb-based scintillators have been undertaken in view of the potential for these scintillators in the detection and measurement of neutrinos as well as general applications in radiation detection and measurement (Belogurov et al., 2003, 2004; Chipaux et al., 2002; Ricci et al., 2011).

Other potential inorganic scintillators for the detection and measurement of neutrinos are the indium-based crystal scintillators (Borisevich et al., 2005; Hsiao and Chang, 2011). Inverse beta decay with ^{115}In was first proposed by Raghaven (1976) for the detection and measurement of neutrinos. The inverse beta decay in nuclei of ^{115}In would occur in indium-based crystal scintillators as follows:

$$\nu_e + {}^{115}_{49}In \rightarrow {}^{115}_{50}Sn^* + e^- \quad (16.51)$$

The superscript asterisk in Eqn 16.51 denotes an excited state of ^{115}Sn, which decays to the ground state with a lifetime of 4.76 μs and emits two γ-ray photons of 116 and 497 keV. This provides a triple-coincidence signal, namely the emitted electron together with the two γ-ray photons (Fukuda et al., 2010).

Elements

William F. Bleam, in Soil and Environmental Chemistry, 2012

1B.2 Nuclear Fusion

The early universe was very hot and dense—ideal conditions for nucleosynthesis but short-lived because the universe was also rapidly expanding. Rapid expansion cooled the early universe to temperatures that could no longer sustain nuclear fusion within a few minutes after the Big Bang. The composition of the universe was limited to the handful of elements that formed during the early minutes of its existence until about 100 million years later (Larson and Bromm, 2001), when the first stars formed and the second stage of stellar nucleosynthesis began.

Primordial nucleosynthesis began a fraction of a second after the Big Bang, when the temperature of the universe had dropped to 10^9 K, low enough for protons to capture neutrons, forming hydrogen isotopes and heavier elements through nuclear fusion. The absence of stable isotopes with *A* = 5 and *A* = 8 (black boxes on diagonal, Figure 1A.3) created a bottleneck for primordial nucleosynthesis beyond ^7_3Li and ^7_4Be.

Free protons and electrons are stable, but neutrons can survive only 10.3 *m* in an unbound state. The neutron-capture rate drops as the temperature of the expanding universe cools below 10^9 K, resulting in the decay of unbound neutrons to protons, electrons, and electron antineutrinos $\bar{\nu}_e$, bringing primordial nucleosynthesis to a close.

$${}^1_0n \xrightarrow{t_{1/2} = 10.3\,m} {}^1_1H + {}^0_{-1}e + \bar{\nu}_e$$

About 100–250 million years after the Big Bang, gravitational collapse of gas clouds led to the first generation of stars (Larson and Bromm, 2001). The core temperature in collapsing gas clouds rose until, once again, they reached about 10^9 K.

A collapsing gas cloud emits infrared radiation as its temperature rises. Radiation emission is a cooling process that controls the eventual size of the star. Population III (first-generation) stars did not cool as efficiently as later-generation stars because they lacked heavy elements. As a result, Population III stars with masses of 100 solar masses or higher were much more common (Larson and Bromm, 2001). Massive Population III stars meant that supernovae were more common—a star must have a mass greater than 9 solar masses to produce a core-collapse or Type II supernova.

The Sun derives 98 to 99% of its energy output by the so-called *proton-proton I cycle,* depicted in the following reactions:

H11+H11→nuclearfusionH12+e+10+veH12+H11→nuclearfusionH23e+γH23e+H23e→nuclearfusionH24e+2H11

The intermediate isotopes in these reactions—H12 and H23e—do not accumulate. The net product of the *proton-proton I* process is production of alpha particles:

4H11→netH24e+2e+10+2ve+γ26.7MeV

Regardless of the specific process, the temperatures in the stellar core produced by hydrogen burning are insufficient to fuse alpha particles into heavier elements. Hydrogen burning ceases once nearly all of the hydrogen in the stellar core is gone and gravity causes the core to collapse. This second collapse increases core temperatures above 10^9 K, sufficient for a second stage of stellar nucleosynthesis: helium burning.

A sequence of nuclear fusion reactions unfolds as heavier elements form and burn at ever-increasing temperatures as the stellar core continues to collapse (see Appendixes 1A and 1C). Each collapse and core temperature increase makes it possible to fuse heavier nuclei that resist fusion at lower temperatures. The sequential fusion of alpha particles with heavier nuclei tends to produce isotopes with even atomic numbers *Z* and mass numbers *A* of 32, 36, 40, 48, 52, and 56. About 97% of the stars in our galaxy lack sufficient mass to sustain fusion reactions beyond the *triple-alpha process* (see Appendix 1C). These stars evolve into white dwarfs and do not eject heavy elements into interstellar space. Stars exceeding 9 solar masses undergo a series of collapses, leading to higher temperatures and densities capable of sustaining carbon, oxygen, and silicon burning. Each stage is less efficient, producing less energy and fewer nuclei. The fusion reactions in this sequence are all exothermic up to F2656e. The final collapse of these massive stars triggers a *core-collapse* or *Type II* supernova (Figure 1B.1), seeding the interstellar medium with dust containing heavy elements that eventually collapse to form second-generation *Population II* stars.

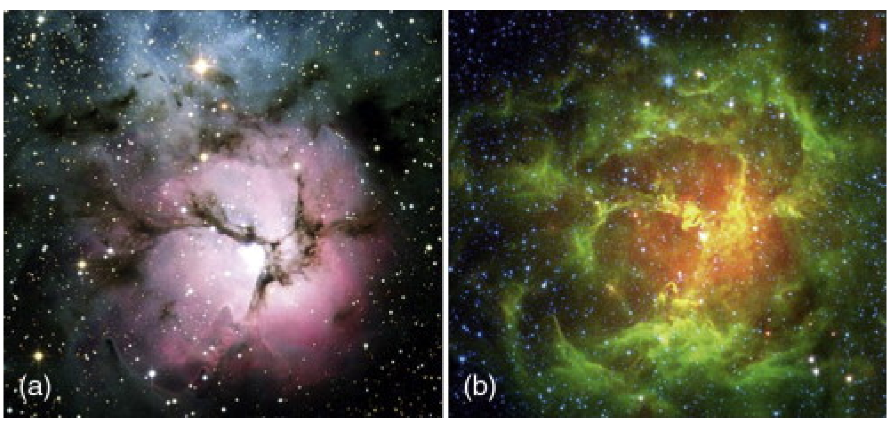

Sign in to download full-size image

Figure 1B.1. False color images at two wavelengths of the Trifid Nebula.